Strike-slip faulting as a trigger mechanism for overpressure release through piercement structures. Implications for the Lusi mud volcano, Indonesia

A. Mazzini [a,*], A. Nermoen [a], M. Krotkiewski [a], Y. Podladchikov [a], S. Planke [a,b], H. Svensen [a]

[a] Physics of Geological Processes, University of Oslo, Sem Sælandsvei 24, Box 1048, 0316 Oslo, Norway
[b] Volcanic Basin Petroleum Research, Oslo Research Park, 0316 Oslo, Norway

ABSTRACT

Piercement structures such as hydrothermal vent complexes, pockmarks, and mud volcanoes, are found in various geological settings but are often associated with faults or other fluid-focussing features. This article aims to investigate and understand the mechanisms responsible for the formation of piercement structures in sedimentary basins and the role of strike-slip faulting as a triggering mechanism for fluidization. For this purpose four different approaches were combined: fieldwork, analogue experiments, and mathematical modeling for brittle and ductile rheologies. The results of this study may be applied to several geological settings, including the newly formed Lusi mud volcano in Indonesia (Mazzini et al., 2007).

Lusi became active the 29th of May 2006 on the Java Island. Debates on the trigger of the eruption rose immediately. Was Lusi triggered by the reactivation of a fault after a strong earthquake that occurred two days earlier? Or did a neighbouring exploration borehole induce a massive blow-out? Field observations reveal that the Watukosek fault crossing the Lusi mud volcano was reactivated after the 27th of May 2006 earthquake. Ongoing monitoring shows that the frequent seismicity periodically reactivates this fault with synchronous peaks of flow rates from the crater. Our integrated study demonstrates that the critical fluid pressure required to induce sediment deformation and fluidization is dramatically reduced when strike-slip faulting is active. The proposed shear-induced fluidization mechanism explains why piercement structures such as mud volcanoes are often located along fault zones.

Our results support a scenario where the strike-slip movement of the Watukosek fault triggered the Lusi eruption and synchronous seep activity witnessed at other mud volcanoes along the same fault. The possibility that the drilling contributed to trigger the eruption cannot be excluded. However, so far, no univocal data support the drilling hypothesis, and a blow-out scenario can neither explain the dramatic changes that affected the plumbing system of numerous seep systems on Java after the 27-05-2006 earthquake. To date (i.e. April 2008) Lusi is still active.

1. Introduction

Mud volcanoes are known to be associated with faults in active tectonic settings (e.g. Brown, 1990; Kopf, 2002, 2008; Bonini, 2007). Due to the short duration of the mud volcano eruptions, studies on how faulting and seismicity affect these eruptions are commonly missing. However, the May 2006 eruption of Lusi in Indonesia is still ongoing and provides a unique opportunity to study the relationship between faulting and mud volcanism. Moreover, Lusi represents an exclusive event to study the triggering and formation of a mud volcano eruption from its birth.

The 29th of May 2006 a sudden eruption of 100 °C mud and gas started in NE Java (Mazzini et al., 2007). This event marked the birth of the mud volcano named Lusi (i.e. Lumpur-Sidoarjo), located along the major Watukosek strike-slip fault zone. The eruptions of mud volcanoes normally last a few days, whereas the Lusi eruption surprisingly continued and escalated. After three days, the flow rate from Lusi reached 50,000 m^3/day rising to a record high of 180,000 m^3/day at the end of September 2006. The mud flow currently covers an area of ~7 km^2 although large amount of mud is constantly diverted to the neighbouring Porong river. About 40,000 people have been displaced and the mud volcano is still active after nearly 3 years. Lusi seems to be unstoppable, and all the attempts to halt the mud eruptions have so far failed (Mazzini et al., 2007).

Both the scientific and the social aspects of Lusi initiated a search for eruption triggers. Mazzini et al. (2007) provided the

* Corresponding author.
  E-mail address: adriano.mazzini@fys.uio.no (A. Mazzini).

first detailed documentation of the geological setting, the regional stratigraphy, as well as analyses and interpretation of the solids and the fluids erupted from the volcano and the neighbouring (200 m) Banjar Panji 1 (BJP1) exploration well. The temperature of the erupted mud reaches 100 °C and may even be higher in the central part of the crater. Although Lusi is located close to the volcanic arc, so far fluid geochemistry does not indicate the involvement of magmatic fluids. The origin of the solids and fluids can be traced to sedimentary strata between ∼1300 and 1870 m depth.

Of key importance for understanding the birth of Lusi is a 6.3 M earthquake that struck the southern part of Java (southwest of Yogyakarta, ∼250 km away from Lusi) about two days before the eruption (U.S. Geological Survey, 2006). Was the earthquake altering the plumbing and tectonic system in the NE of Java? We have previously suggested, based on field and geochemical data, that the earthquake could have triggered the Lusi eruption by reactivating the Watukosek fault and a sub-surface piercement structure, subsequently releasing overpressured fluids (Mazzini et al., 2007). An alternative hypothesis linked the initiation of Lusi to a blow-out of the nearby BJP1 exploration well (Davies et al., 2008; Tingay et al., 2008).

In order to better understand the Lusi events and the controversy related to its formation, we present new field observations that highlight the activation of the Watukosek fault after the May 2006 earthquake. These data are complemented by a multidisciplinary approach that integrates laboratory experiments with mathematical modeling covering the rheological end members. The combination of these complimentary methods may constrain the triggering of the Lusi eruption and further explore the earthquake-fault scenario (Mazzini et al., 2007) as a trigger for the Lusi eruption. In this paper we also distinguish between the causes (all the geological events predisposing the Lusi system) and the triggers (the final initiating events) of the eruption. The ultimate purpose is to establish the relationship between tectonic deformation and critical fluid pressure at which eruptions occur in settings prone to mud volcanism.

2. Methods

2.1. Fieldwork

Three field campaigns to the Java Island were undertaken in 2006, 2007, and 2008. The fieldwork was done around the Lusi eruption site and in the surrounding areas towards the NE (e.g. Sidoarjo and Renokenongo villages). Further fieldwork was done along the Watukosek fault zone and towards the neighbouring Arjuno volcanic complex where the fault originates. Mud volcanoes were studied along the Watukosek fault, and further to the NE, on the Madura Islands, and in central Java along an EW trending major anticline (Figs. 1 and 2).

2.2. Analogue experiment setup

A 3D experiment was designed to study the relationship between a) the imposed tectonic forcing during strike-slip movement, b) the critical fluid pressure to trigger an eruption, and c) the surface observation of fluidization and the formation of piercement structures. The setup consisted of a 1 × 1 × 1 m plexiglas box with a circular 40.5 cm diameter air inlet at the base (Fig. 3A). The inlet was covered with a rigid metal mesh that allowed air to be flushed through without the powder clogging the inlet. Half of the inlet surface was covered with a movable plastic mesh. A layer of granular material was placed above this mesh. Several layers of granular material were used during the experiments, varying from 2.5 to 5.2 cm in thickness. Three different types of granular media with

contrasting properties were used: 1) cohesive devolite clay (China clay) with low permeability, 2) cohesionless silica spheres with a diameter of 0.05 ± 0.01 mm with low permeability, and 3) cohesionless glass beads with a diameter of 0.28 ± 0.1 mm and high permeability. Air was flushed through the system via the inlet at the base, creating a slight overpressure in the granular bed. The applied air pressure was below the threshold of fluidization and did not create any observable perturbation on the external surface of the bed. The movable plastic mesh, covering half the air inlet, was then shifted horizontally by 1–2 cm inducing a strike-slip movement within the overlaying bed. The shearing triggered fluidization of the media. The surface was monitored using a high resolution B&W Jai CV-M7 digital camera with a Nikon FM Nikkor 20 mm lens, recording 20 pictures per second. The pressure data were collected in real time by an Omega PX139-004 DV pressure sensor. The pressure sensor was placed within the air inlet beneath the base of the box. A Labview software simultaneously logged the pressure and image data. The granular media are distributed over a surface of 0.8 × 0.8 m in the central part of the 1 × 1 m plexiglas box. In this way there was no contact with the plexiglas walls that could otherwise influence both the fluid flow and the stress field in the bed.

### 2.3. Mathematical modeling

As a follow up of the analogue experiments, we developed a set of numerical models in order to quantify the relationship between the critical fluidization pressure and the tectonic deformation. Both laboratory and numerical models have similar challenge of establishing the analogy between the rheology used in the experiments and rheological response of natural prototype. Our strategy was to consider the sensitivity, i.e. the rheological dependency, of the strike-slip induced fluidization model. In order to do this we studied three end member rheologies: (1) A ductile model, where the material strength is not sensitive to the solid pressure (von Mises); (2) a brittle model, where the material strength increase with the solid pressure (Mohr-Coulomb); and (3) a bilinear Bingham-like viscous model where the material strength is reduced at a critical stress. Models 1 and 2 are rate independent, whilst model 3 is a creeping, rate dependent viscous model. The critical differential stress at which the material fails is termed the yield stress τ_c.

2.3.1. Brittle rheology

The model focuses on the stress direction defined in Fig. 3B. We have estimated the fluidization potential by linear superposition of fluid overpressure and tectonic stresses and substituting them into three-dimensional von Mises and Mohr-Coulomb yield criteria. The accuracy of such linear superposition approach was recently investigated in two-dimensions by Rozhko et al. (2007).

2.3.2. Ductile rheology

Numerical modeling was used to study the effect of horizontal tectonic deformation on the fluidization of clay (critical fluid pressure ΔP_c) caused by localized fluid overpressure at depth. For this purpose we used a 2D Finite Element incompressible viscous Stokes flow solver for Matlab, MILAMIN (Dabrowski et al., 2008). It is assumed that the clay has a generalized bilinear Bingham fluid rheology with a stress-dependent viscosity, where the viscosity drops at stresses exceeding a critical yield strength τ_c. This is the most common approach to describe the clay rheology (e.g. Imran et al., 2001; Marr et al., 2002). A schematic of the bilinear stress–strain rate diagram of this rheology is presented in Fig. 4A. Note that for infinitely large viscosity μ_1, Fig. 4A represents the classical Bingham fluid rheology. The 2D geometry of the model is
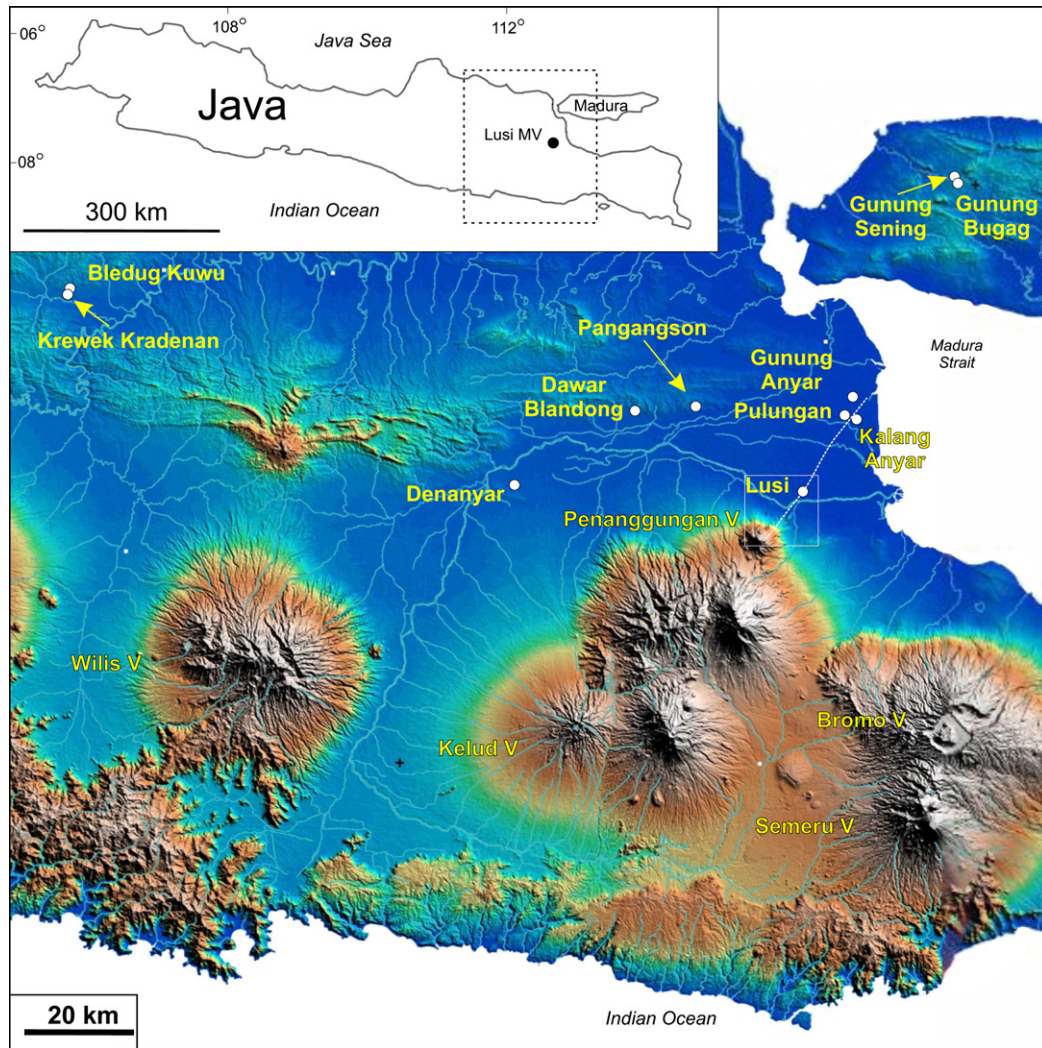
Fig. 1. Fragment of elevation map of eastern Java Island with the location of the discovered mud volcanoes in the backark basin (marked as circles). The Watukosek fault, striking from the Arjuno volcanic complex, crossing the Lusi mud volcano and extending towards the NE of the island, is marked with white dashed line. Magmatic volcanoes are marked with letter V after the name of the structure. Inset shows the Java Island with framed region magnified in the elevation map.

presented in Fig. 4B. The box containing the Bingham fluid was subjected to horizontal deformation. In a small region of width w we specified a non-zero vertical stress boundary condition ΔP representing a central overpressured fluid source. A geological analogue for this setting can be the tip of the overpressured diapir (e.g. similarly to what observed at Lusi site in seismic images, see following). Since the initial flat topography and the homogeneous densities do not induce any differential stresses, gravity effects were considered negligible. The other parameters were the height h and length l of the domain. Free surface boundary conditions were imposed at the top of the domain. Along the sidewalls and the bottom boundary the shear stresses were set to zero ($\sigma_{xy} = 0$). This implies that the sidewalls could move freely in vertical direction, but were fixed in the horizontal direction. The bottom boundary was free to move horizontally, but not vertically (except for the inlet region). Both the overpressure at the inlet, and the horizontal deformation induce differential stresses that affect the material viscosity according to formula (1) (See Appendix 1). Our numerical study is a quantification of the critical conditions at which the material transforms from having a solid-like to a fluid-like behaviour under tectonic loading. See Appendix 1 for further details on the numerical modeling.

3. Results

3.1. Field data

The Watukosek fault zone cuts Lusi and the northeastern part of Java with an SW–NE orientation. This fault (Figs.1 and 2) strikes from the Penanggungan volcano, outcrops along the Watukosek escarpment, and, further to the NE, alters the course of the Porong river creating a sharp bend towards the north. The fault zone continues its course towards the Madura Island accommodating the Lusi, Gunung Anyar, Pulungan, and Kalang Anyar mud volcanoes. On Java, additional mud volcanoes have been inferred from satellite images along this lineament. Following the same trend the Gunung Sening and Gunung Bugag mud volcanoes are present in the Madura Island (Fig. 1). Further evidence of the fault appears close to the delta of the Surabaya River where the river has a sharp turn and, further to the east, forms an embayment along the coast.

Was the Watukosek fault system reactivated after the 27th May 2006 earthquake? And most importantly what is the physical link between the fault and the Lusi eruption? Here we summarize key data from our fieldwork together with the eruption chronology:
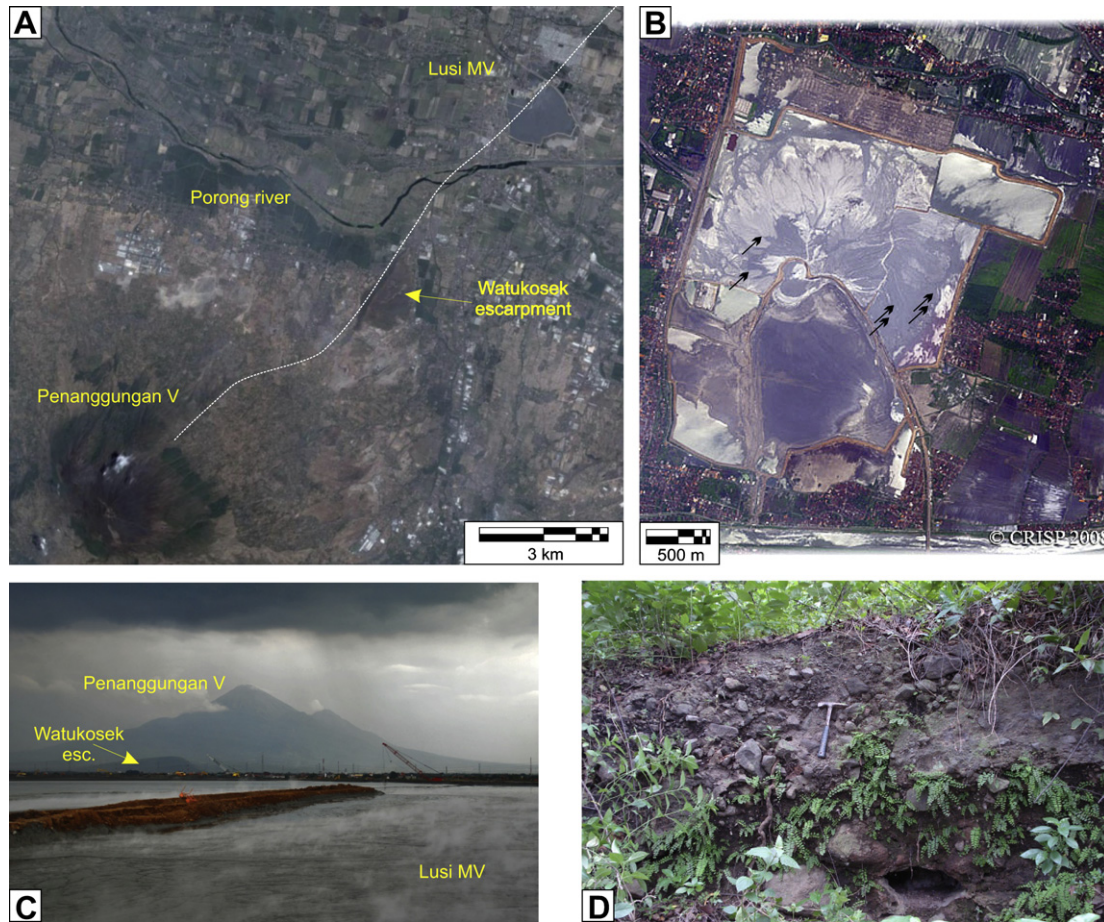
Fig. 2. (A) Satellite image of the area around Lusi (framed in white in Fig. 1) showing the Penanggungan volcano to the SW, the escarpment where the Watukosek fault outcrops, the bending of the Porong river, and the Lusi mud volcano. A dashed line marks the direction of the fault, based on field and satellite observations. Satellite image from Google Earth. (B) Ikonos satellite image of Lusi the 12th of December 2008. Courtesy of Crisp, NUS 2008. Black arrows indicate the orientation of the fractures observed before the mud eruption covered the area. (C) View of the Penanggungan volcano on the background seen from the Lusi crater. The Watukosek escarpment is visible in front of the Penanggungan volcano. (D) Strike-slip faulting at the Watukosek escarpment (courtesy A. Clarke).
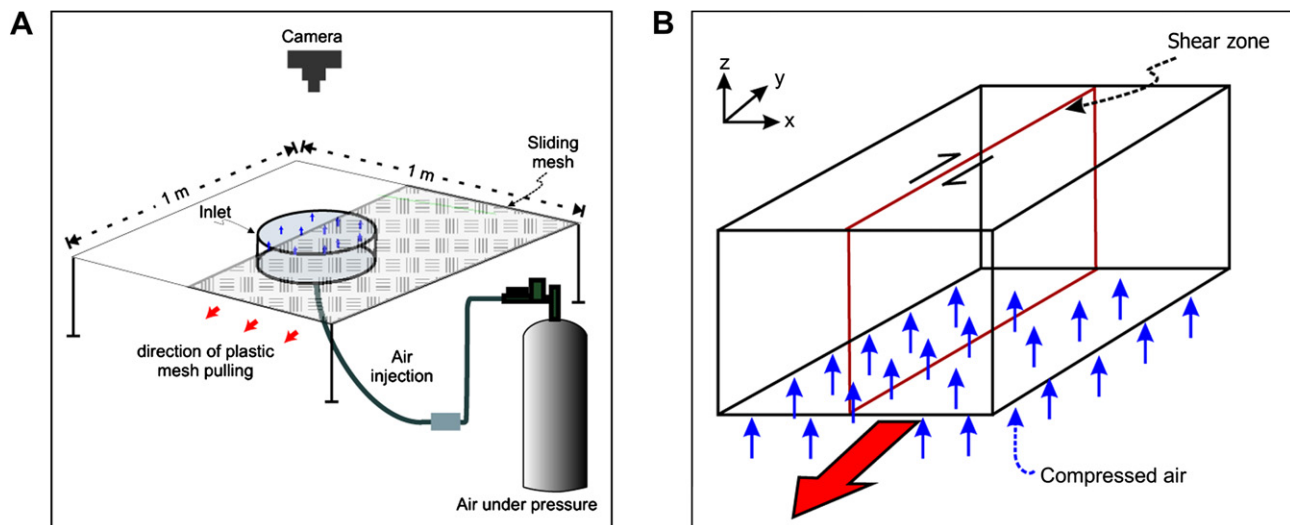
Fig. 3. (A) Analogue experimental setup. A tank of pressurized air is connected to a wide circular inlet with a diameter of 40.5 cm placed inside a 1 × 1 m sized box. A movable plastic mesh that can be pulled along the base of the box surface and induce shearing of the overlaying granular media was placed above the inlet. (B) Simplified sketch of the central zone of the experimental setup in image (A) to define the direction of shear stress along the plane *xy* (in red) and the normal stresses in the *xyz* directions. (For interpretation of the references to colour in this figure legend, the reader is referred to the web version of this article.)

A

B
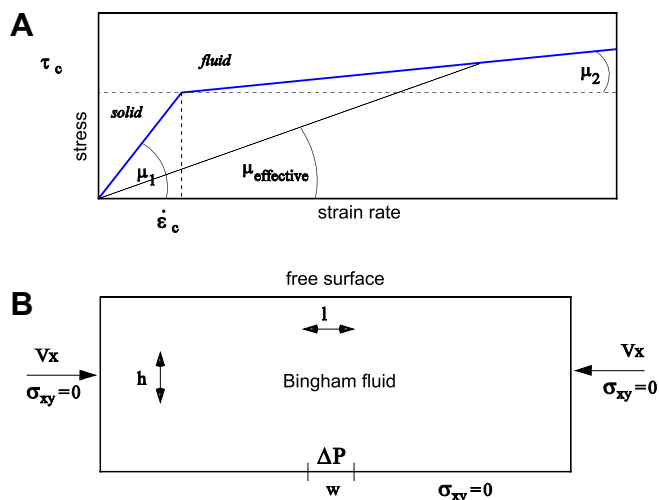
Fig. 4. (A) Plot of the generalized bilinear Bingham fluid rheology. Up to a critical value of differential stress τ_c the material has large viscosity μ_1. For higher stresses the viscosity drops to μ_2. Effective viscosity used in the numerical code $\mu_{effective}$ is computed according to Equation (9). (B) Numerical model setup: a box of length l, height h, containing a Bingham fluid. The model is deformed at the sides with horizontal velocity Vx. In the middle of the bottom boundary there is a region of width w with non-zero vertical stress boundary conditions ΔP simulating a localized overpressured zone.

- Residents close to the Gunung Anyar, Pulungan, and the Kalang Anyar mud volcanoes, located along the Watukosek fault almost 40 km NE of Lusi (Fig. 1), reported increased venting activity of the mud volcanoes after the Yogyakarta seismic event. Simultaneously, boiling mud suddenly started to erupt in Sidoarjo, later forming the Lusi mud volcano.
- A 1200 m long alignment of several erupting craters formed during the early stages of the Lusi eruption, see Figs. 3B and 4 in Mazzini et al. (2007). The direction of these aligned craters coincides with the Watukosek fault. The craters were formed during May-early June 2006, but were later covered by the main Lusi mud flows.
- Large fractures several tens of centimetres wide and hundreds of meters long were observed in the proximity of the BJP1 exploration well with identical NE–SW orientation. However no fluids were observed rising through these fractures suggesting a shear movement rather than a deformation from focussed fluid flow.
- Several NE–SW oriented fractures were reported in early June 2006 in the Sidoarjo village (Fig. 2B).
- The intersection of the fault with the nearby railway clearly indicates lateral movement. The observed lateral movement recorded at the railway during the first four months was ∼40–50 cm. The lateral movement recorded at the neighbouring GPS stations during the same time interval reveals at total displacement of ∼25 cm (2 cm in July, 10 cm in August, 10 cm in September). This later displacement is possibly related to gradual collapse of the Lusi structure. In any case, the difference between these two records shows that remains an initial 15–20 cm of displacement that must have occurred during the early stages (i.e. end of May–June) related to the Watukosek fault shearing. Since the bending started, after the 27th of May earthquake, the rails had to be repaired four times. Two of these repairs were done within the first three months after the earthquake attempting to remove the bending due to the continuous shearing. Note that neither the rails nor the water pipeline (see next bullet) had kink problems before the earthquake.

- A local water pipeline experienced significant bending and ruptures at the intersection with the fault (Fig. 5A–B). Since the May 2006 earthquake occurred, the pipeline has been repaired sixteen times.
- Before the mud flow, the continuation of the fault could be observed to the west and along the main road to the northeast of the Lusi crater and, even further to the northeast, inside the Sidoarjo and the Renokenongo villages (Figs. 2 and 5C–D). Here the fractures could be observed showing lateral shearing in early June.
- The ongoing collapse in the Lusi region has an ellipsoidal shape that follows the direction of the Watukosek fault showing that this is a weakness zone (Sawolo et al., 2009; Fukushima et al., in this issue; Istadi, 2009).

3.2. Seismic data

Seismic profiles collected during the 1980s, crossing the actual Lusi eruption site, show a kilometer-sized dome-shaped structure in the uppermost ~3 km (to about 3 s; Fig. 6A, B). The central part of the dome is characterized by disrupted seismic reflections. The structure is interpreted as a piercement complex, with a central conduit of mobilized, gas-charged sediments.

The piercement structure is not imaged on seismic profiles 1–4 km to the north and south of Lusi (Fig. 6C, D). However, a prominent NE–SW oriented anticline and fault system, the Watukosek fault system, can be clearly observed. It is difficult to interpret the geometry of individual fractures and faults, but the faults resemble a flower structure characteristic of strike-slip fault zones. Piercement structures are elsewhere often associated with anticlines in provinces with rapid sedimentation, e.g. mud volcanoes in Azerbaijan and in Pakistan (Planke et al., 2003; Delisle, 2004; Mazzini et al., 2009).

Buried piercement structures are also observed in other seismic lines towards the north of the Java Island. These are interpreted as diapirs and mud volcanoes. One of the most spectacular is the collapse structure that is visible through the Porong 1 well (see Istadi, 2009). This structure likely represents an extinct mud volcano that, once it terminated its activity, gradually collapsed around a vertical feeder channel. Interestingly, mud volcanoes have also been recognized offshore to the northeast (Istadi, 2009).

3.3. Analogue modeling results

Analogue experiments were performed to simulate the correlation between localization of the tectonic shear and the formation of piercement structures. During the experiments an initial overpressure was applied through the three different granular media (see Methodology) without inducing fluidization or causing perturbations in the upper surface. The three experimental series gave comparable results: a limited (∼1 cm) shearing applied to the system was sufficient to trigger a sudden localized fluidization along the shear zone. Fluidization occurred almost simultaneously to the imposed shearing and the events were too fast to be seen by eye.

Tensile and shear fractures formed in the cohesive China clay during shearing, immediately following the initial mm-scaled displacement. Small seeps initially distributed along these cracks before a more vigorous seepage burst along the main shear zone (Fig. 7A). No tensile fractures were observed while shearing the cohesionless glass beads (diameter = 0.28 mm). A sudden pressure drop was recorded during the shearing and the formation of a seep within the shear zone (Fig. 7B). Shearing of the cohesionless silica spheres (diameter = 0.05 mm) revealed initial subparallel tensile
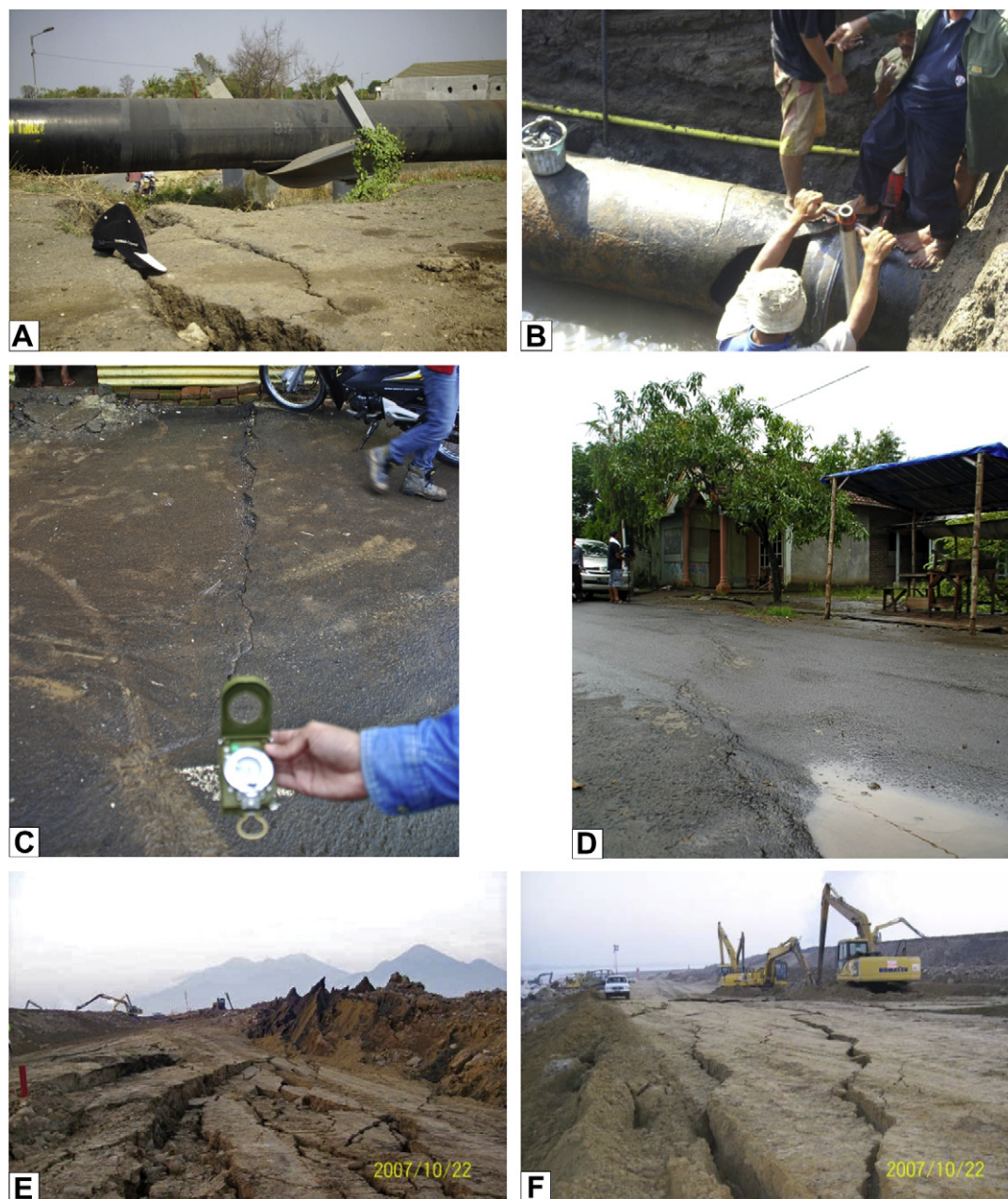
Fig. 5. (A–B) Water pipelines crossing the fault had to be repaired several times after the 27th of May 2006 earthquake. No bending or cracking of the pipelines were observed before the earthquake. (C–D) The fault can be followed moving to the northeast of the Island; (E–F). The reactivation of the Watukosek fault after the fall 2007 earthquakes (see more details in text) shows that even distant seismicity still affects the regional tectonics. Note the significant lateral and vertical movement of the displacement. The Penanggungan volcano can be seen in the background.

bands and an abrupt localized fluidization of the media occurred along the displacement surface resulting in seepage on the surface (Fig. 7C).

3.4. Brittle rheology results

Mohr-Coulomb and von Mises failure yielding mechanisms were used to investigate the effect of the tectonic stress on the critical fluidization pressure. Both approaches reveal similar results. Only a detailed description of the von Mises derivation criterion is given, while the Mohr-Coulomb follows the same line of derivation. A more detailed description of the results and calculations are provided in Appendix 2.

Fig. 8 plots the derived analytic functions for the critical pressure using the von Mises criterions eqn. (6) and the Mohr-Coulomb criterion eqn. (8). The results show that the critical fluid pressure for fluidization, ΔP_c is reduced for increasing values of shear stresses σ_{xy}. The presented model predicts that a shear stress of, e.g. 90–95% of the yield stress reduces the critical pressure by a factor 1.5–2 and 2.5–5 for the Mohr-Coulomb and von Mises model, respectively.

3.5. Ductile rheology results

Two cases were studied to model the mechanism of fluidization: a static case and a horizontal deformation case.
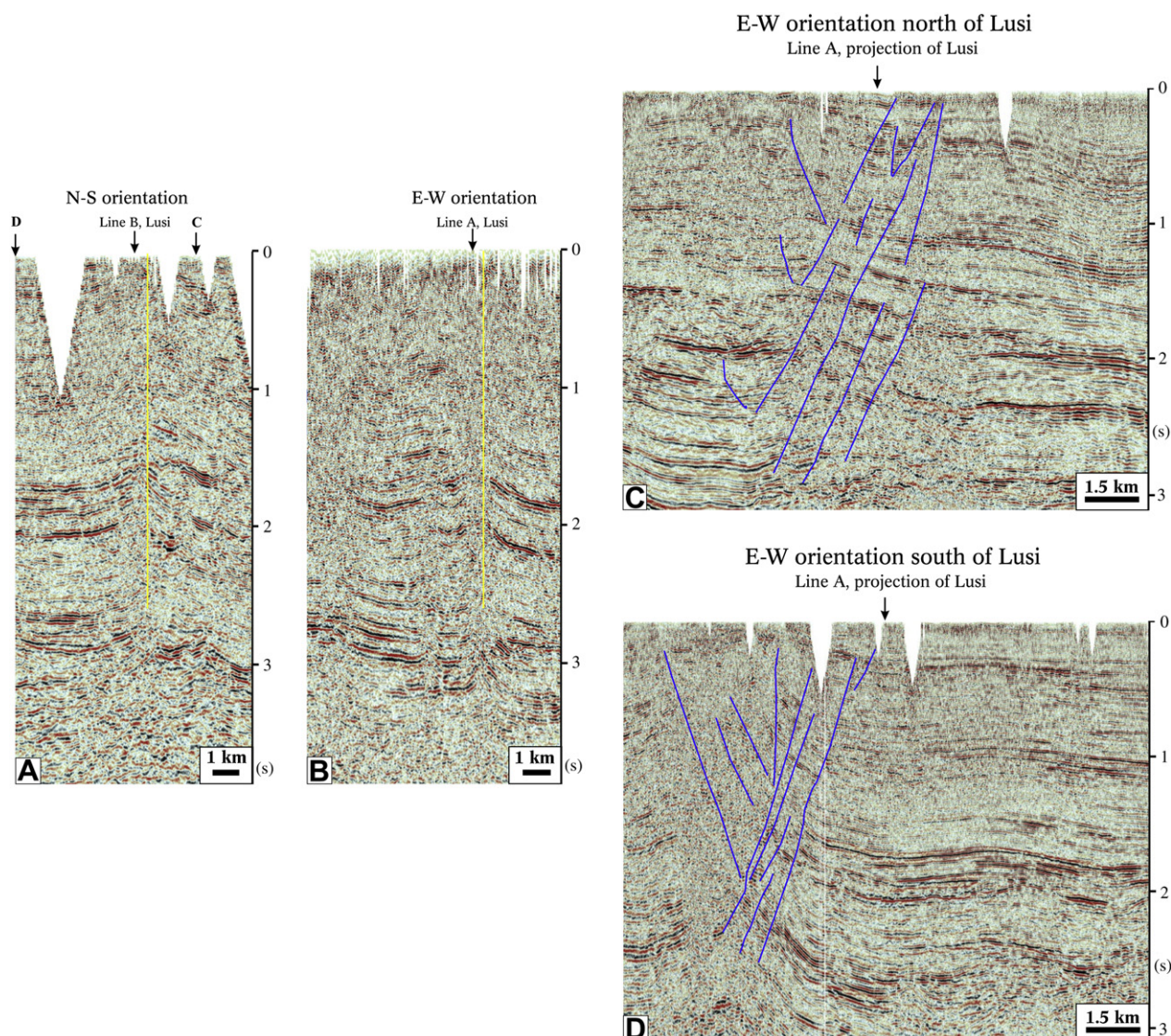
Fig. 6. Seismic profiles acquired prior to the Lusi eruption. (A) N–S and (B) E–W oriented profiles crossing the Lusi mud volcano. Both profiles show the presence of a dome at 1.5–2.5 s. The dome was drilled by the BJP1 exploration well (yellow line), and is interpreted as a pre-existing piercement structure. (C) and (D) E–W oriented profiles located ∼1.5 and 4 km north and south of the Lusi mud volcano. Both profiles show the Watukosek fault zone (schematically shown as blue lines) that originates at the Arjuno volcanic complex and continues to the NE part of Java. (For interpretation of the references to colour in this figure legend, the reader is referred to the web version of this article.)

### 3.5.1. Reference experiments: the static case

In order to get a better understanding of the controlling parameters of the experimental setup, the first experiments were performed with zero horizontal velocity at the side boundaries ($V_x = 0$). We verified that the boundary effects were negligible, since the box length l was much larger than the height. Fig. 9A shows effective viscosity profiles for different values of ΔP. Increasing fluid overpressure at the inlet led the formation of a low viscosity fluidized channel zone. This newly formed conduit, extending from the bottom of the model to the surface, forms an elevated flow velocity with a given fluid overpressure at depth. In a geological analogue, this effect could result in a localized mud channel and finally lead to an eruption. When the low viscosity channel breaches the surface we define the system to be fluidized.

In this set of numerical experiments we measured the critical overpressure ΔP required to reach the fluidization criterion. We refer to this value as ΔP_c. We then investigated the effect on ΔP_c of a varying inlet width, box height, and four orders of magnitude in viscosity contrast. In all these cases, the shape and size of the

created pathways were similar. The results were plotted using ΔP_c scaled by the material yield strength τ_c versus a product of the viscosity ratio μ_1 over μ_2 times the square of the ratio of the inlet width w and model height h. Fig. 9B, C shows that all the data for all numerical experiments collapsed onto a single master curve of varying yield stresses, viscosity contrasts and aspect ratios. Two regimes were obtained as described in the Appendix 3.

3.5.2. Fluidization with horizontal deformation

Further simulations were performed in order to observe the influence of non-zero horizontal velocities V_x at the lateral box boundaries on ΔP_c. For this purpose, a different fluidization criterion was used. ΔP was increased until the effective viscosity in the middle of the model (at $h/2$) dropped by a factor α, i.e. $\mu_{\text{effective}}|h/2 = \alpha\mu_1$. This way of defining the onset of fluidization is one of several possible choices to measure the critical pressure. We used it since it provided an easy algorithmic way to define the fluidization criterion for varying model parameters (e.g. boundary velocities, viscosity contrast, model height).
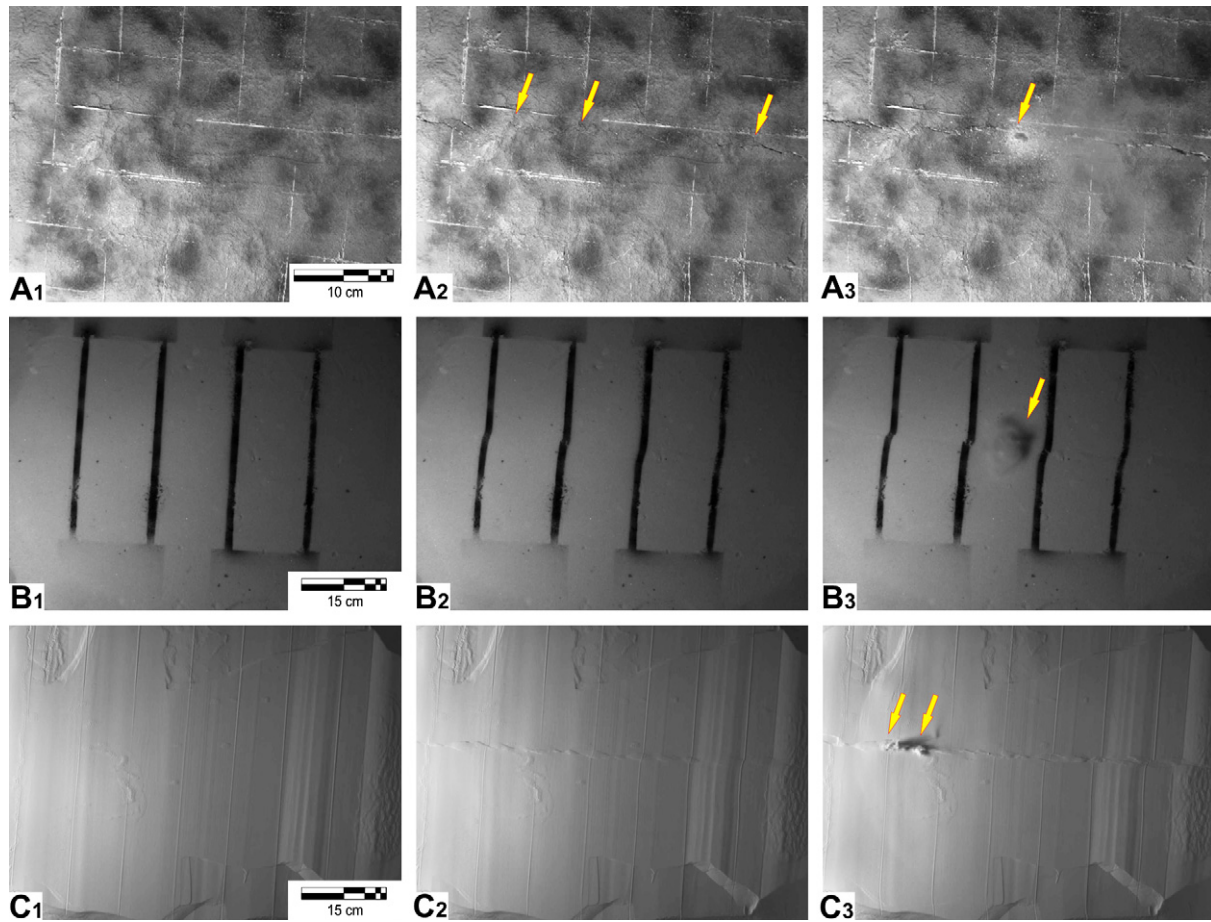
Fig. 7. Analogue shearing experiments of overpressured granular media. (A1) Initial experiment setup using high cohesive China clay; (A2) beginning of shearing and occurrence of tensile cracks; seepage of air occurs along the tensile cracks (arrowed); (A3) shearing continues and a vigorous burst occurs along the sheared zone (arrowed). (B1) Initial experimental setup using cohesionless glass beads; (B2) beginning of shearing; (B3) sudden burst along the sheared zone (arrowed). (C1) Initial experimental setup using cohesionless silica spheres; (C2) beginning of shearing and the formation of tensile cracks propagating from the sheared zone; (C3) sudden burst along the sheared zone (arrowed).

Fig. 9D shows the computed ΔP_c in the $(\frac{w}{h})^2 \ll \frac{\mu_2}{\mu_1}$ regime (see Appendix 3 for the choice of the regime) scaled by the fluidization parameter α and the parameters obtained from the static study. The *x*-axis is the imposed background stress over τ_c, where negative values denote compressional, and positive values denote extensional boundary velocities. In the absence of the overpressure source, values of $+1$ and -1 on the *x*-axis would imply material failure in the entire domain caused by horizontal deformation only. For different values of α and a wide range of viscosity contrasts we get a data collapse for the measurements of ΔP_c at any given horizontal deformation.

Fig. 9D can be interpreted as the fluidization condition in the presence of tectonic deformation and is similar to the diagrams calculated by Rozhko et al. (2007) for brittle rheology. Our results define two distinct regions: a) the region below the curve represents the *stable* regime (i.e. when the fluid overpressure at depth does not result in the formation of an eruption); b) the region above the curve is *unstable* (i.e. the values of overpressure at depth and boundary velocities together are sufficient to cause the material fluidization and eruption).

In the case of the extensional regime, any increasing tectonic stress results in an efficient drop of the critical pressure at fluidization ΔP_c (Fig. 9E). This means that in the presence of extensional boundary velocities, the critical overpressures at depth required to fluidize a part of the model are reduced.
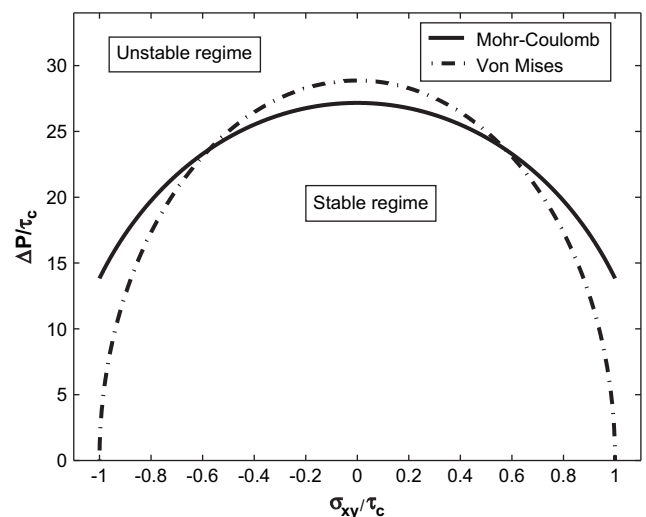
Fig. 8. Plot of the model for the critical fluid pressure as a function of the imposed shear stress. Both axis are normalized by the yield strength for the Mohr-Coulomb criterion and the von Mises failure criterion, equations (8) and (6) respectively. For the Mohr-Coulomb estimate the cohesion *C* is replaced by τ_c. The analytic estimate shows that non-zero shear stresses decrease the critical fluid pressure at which fluid induced deformation occurs. In the plot the gravity was neglected, the coefficient of side friction was set to 0.94 and the internal angle of friction was set to 30°.

In the case of compressional regime, normalized boundary velocities between −0.2 and 0 cause a slight increase in the value of ΔP_c. This implies that in this model larger overpressure values are required to obtain fluidization in this regime. The effective viscosity profiles presented in Fig. 9E suggest that compression first causes horizontal spread and a relative lowering of the fluidized zone. Although the total fluidized volume is increased, more overpressure is needed in order to drop the viscosity to a desired level at the fixed height. Normalized boundary velocities between −1.1 and −0.2, and between 0 and 1, result in a significant drop of ΔP_c.

As noted earlier, in the absence of overpressure large values of the normalized background stress of above +1 or −1 would cause material failure in the entire domain. However, viscosity profiles in Fig. 9E show that if overpressure is present, the failure is localized in a narrow zone, leaving the bulk of the material unaffected.

4. Discussion

The seismic data show that a piercement structure in gas-saturated sediments existed at the Lusi site before the eruption. Regional seismic lines show that an NE–SW oriented faulted zone (Watukosek fault) is crossing the Lusi location. Fieldwork and regional observations provide evidence of the reactivation of this fault after the 2006 earthquake (see also Section 3.1). We propose that the reactivation of the Watukosek fault contributed to alter the plumbing system of the area around the fault. The fault lost its sealing capacity and allowed an expulsion of hot fluids to the surface draining a large volume of the sedimentary units towards the fault plane (Fig. 10).

A similar scenario has been observed in other localities where geological structures such as faults (particularly strike-slip faults) and anticline axis host mud volcano and piercement structures. Classic examples are documented in e.g. Trinidad, Azerbaijan, Pakistan, California, and Italy, (e.g. Jakubov et al., 1971; Dia et al., 1999; Planke et al., 2003; Delisle, 2004; Mellors et al., 2007; Bonini, 2007). However the physical parameters and the mechanisms applicable at these locations have never been studied in detail. Our modeling represents a first step in this direction and is relevant for understanding the possible triggers of the 2006 Lusi eruption.

4.1. Implications from mathematical modeling

The geological data presented so far provide evidence of the reactivation of the Watukosek fault after the 27th of May 2006 earthquake. But what is the effect on a regional scale of this strike-slip event? In order to address this question the data described above was used as the working hypothesis for the analogue and mathematical modeling. The effects of the combined shear stress and strain (typical of strike-slip faults) on the fluidization pressure were studied. These results have applicability not only for the Lusi study case, but for all the settings prone to mud volcanism where strike-slip faulting occurs.

The analogue experiments provide two key observations: a) the fluidization and the formation of the eruptive piercement structures are triggered by the imposed shearing, and b) these vent complexes form along the fault plane. The observed pressure drop at the onset of fluidization indicates that the fluidized points act as a rapid pathway to release the fluids onto the surface. The alignment of the fluidization points along the shear zone indicates that the shearing decreases the apparent strength of the material. Note that in all the experiments the fluidization points were randomly distributed along the shear zone, and no correlation was observed to the central part of the inlet. This also confirms that the fluid

overpressure was homogenously distributed within the inlet, i.e. the localization of the fluidized zones could not be explained by heterogeneities in the fluid pressure field but indeed only by the presence of the shear zone.

The physical parameters of the analogue experiments were investigated using a mathematical approach for brittle and ductile rheologies. The models show that the critical fluid pressure at fluidization is monotonically reduced by the rise of shear stresses up to the yield stress level.

In order to trigger the reactivation of the Watukosek fault system, the tectonic stresses must have reached the yield stress at least in a small volume around the tip of the growing fault. Fluidization yield conditions are met if a significant volume around the fault may be unloaded from the yield stress as the very result of the faulting process. Therefore the degree of unloading around a strike-slip fault determines whether fluidization occurs or not. If we assume that unloading by strike-slip yielding and the reactivation of the Watukosek fault system brings the shear stress level to 90–95% of the yield stress, and by applying this value in brittle (rate-insensitive) model, we predict a drop in the critical fluid overpressure by a factor 1.5–5 (see Section 3.4 and Fig. 8) for both the Mohr-Coulomb and the von Mises rheology.

Further support from these conclusions is coming from the ductile (rate-sensitive) rheology modeling. The results from the static experiment show that the critical fluid overpressure needed for the fluidization is very high (about 10–20 times the threshold stress τ_c). In contrast, the horizontal loading experiments show that the critical fluid overpressure at fluidization is dramatically reduced by extensional and compressional tectonic forces in the 10% proximity to the threshold stress τ_c. We propose that the presence of tectonic stresses acts as an apparent weakening mechanism that reduces the critical fluid pressure.

To conclude, analogue and mathematical modeling demonstrated that: (a) it exists a geometrical association between the shearing and the occurrence of piercement structures; (b) the presence of localized tectonic stress and strain favours the triggering of the fluidization for a given overpressure at depth and eruption along the shear zone; (c) this mechanism gives identical results for the investigated brittle and ductile media that represents the end members of possible rheologies; (d) when shearing is applied due to tectonic forces, the critical fluidization pressure can be reduced up to one order of magnitude (e) to cause fluidization in normal static conditions, unrealistically high overpressure is required. These conclusions are applicable to the Watukosek fault movements observed at Lusi site, explaining the eruption scenario documented in this manuscript.
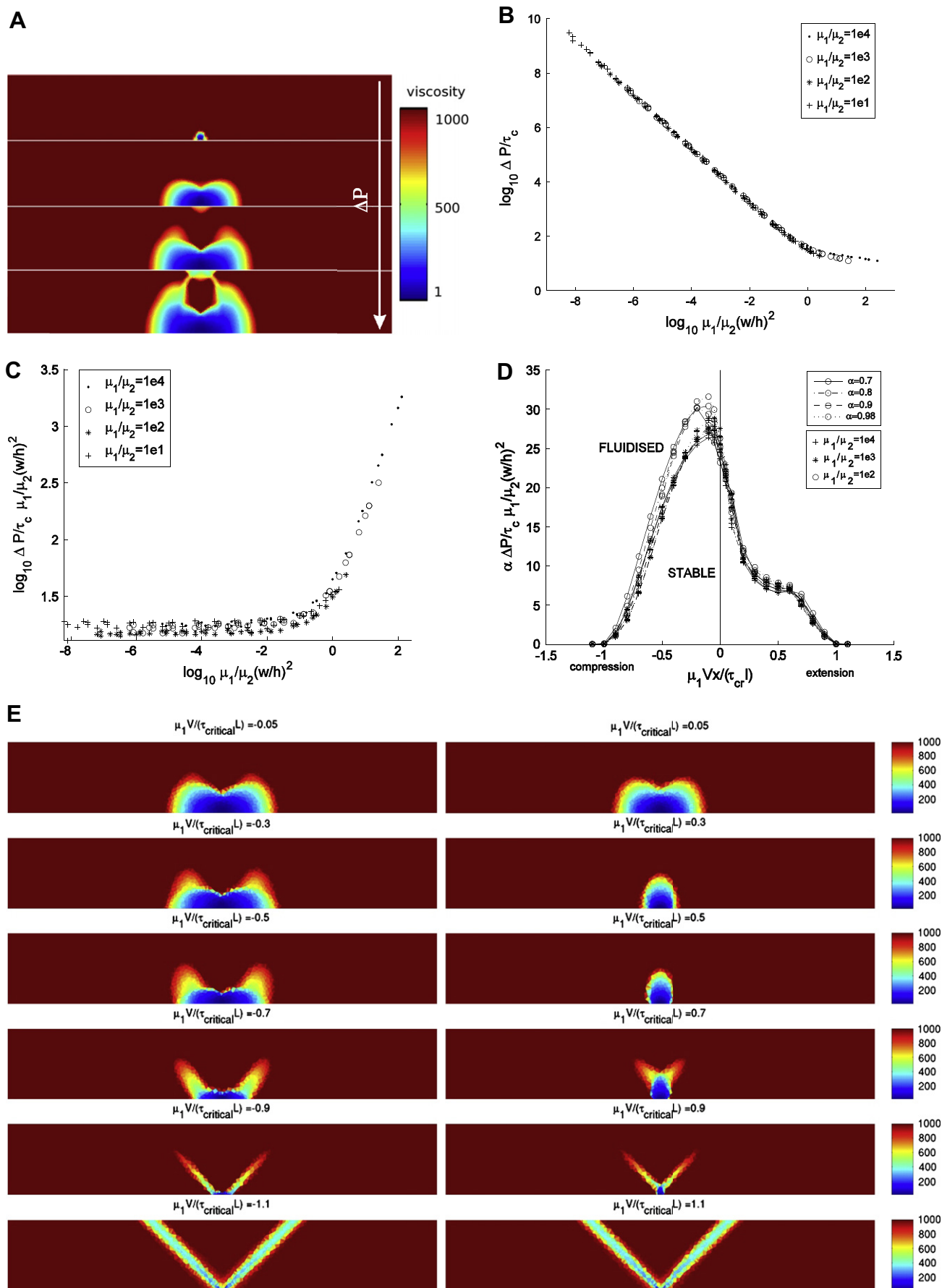
4.2. Causes and triggers

For all the mud volcano eruptions it is essential to distinguish between causes and triggers. The causes represent the sequence of events, geological settings, and external circumstances that have prepared a potential eruption. The trigger is the final step that precedes the manifestation, or the initiation, of an eruption. It is often not sufficient to debate the trigger without first understanding why a volcano system was predisposed to erupt.
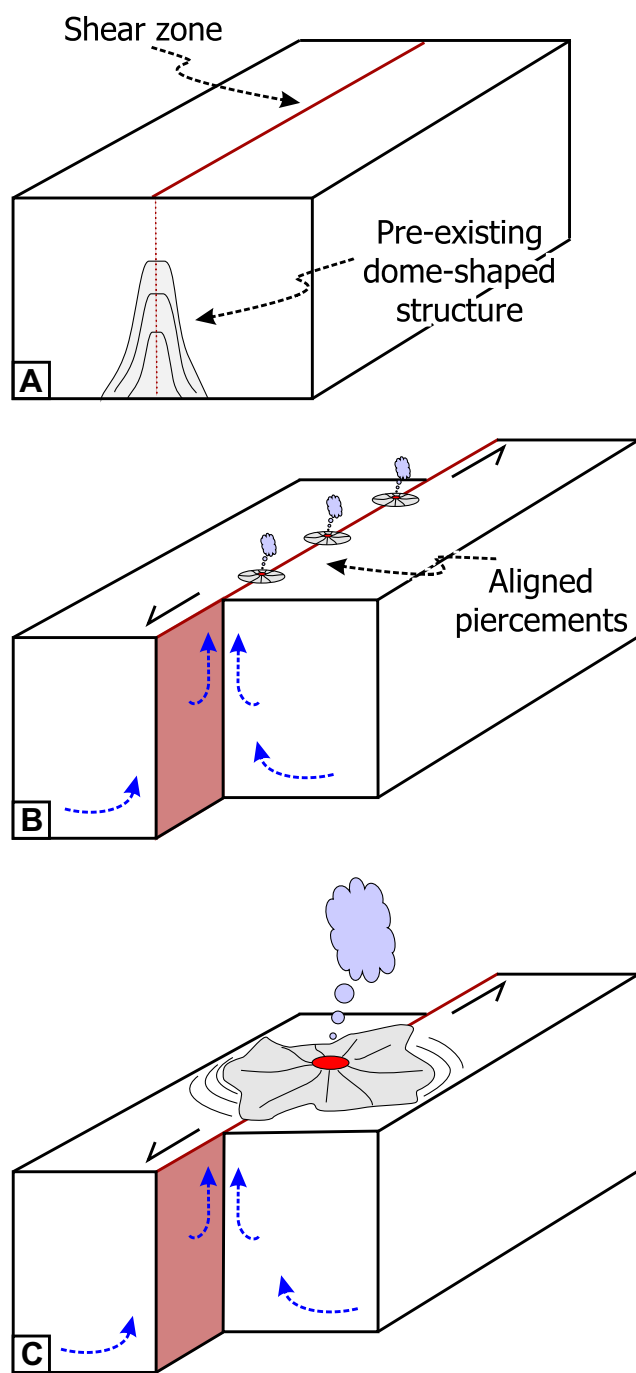
Most of the causes of the Lusi eruption have been already described in the result section; further details are included in Appendix 4. The possible factors contributing as triggers will be discussed in the following sections.

4.3. Triggering: seismicity and piercements

Mud volcano eruptions occur when overpressure at depth is sufficient to fracture the overburden of the overlying sedimentary

units (e.g. Kopf, 2002 and references therein). When a threshold is reached due to continuous generation of fluids (e.g. water, hydrocarbons) at depth, a system of fractures propagates towards the surface breaching the seal. Ultimately, a critical value is reached and large-scale fluidization occurs. The fluidization in sedimentary basins starts when the granular material changes from solid-like to fluid-like behaviour as a consequence of interstitial fluid flow exceeding a critical limit (e.g. Gidaspow, 1994).

The natural process of fracture propagation and fluidization can be accelerated by seismic activity. Shaking from earthquakes may generate fractures that provide a free pathway for deeper fluids. It is well documented that seismic activity enhances the activity of geysers, methane emissions, magmatic volcanoes and mud volcanoes and perturb the plumbing systems at regional scales (Chigira and Tanaka, 1997; Guliev and Feizullayev, 1997; Linde and Sacks, 1998; Delisle et al., 2002; Kopf, 2002; e.g. Hieke, 2004; Nakamukae et al., 2004; Manga and Brodsky, 2006; Ellouz-Zimmermann et al., 2007; Lemarchand and Grasso, 2007; Mau et al., 2007; Mellors et al., 2007; Walter and Amelung, 2007; Judd and Hovland, 2007; Eggert and Walter, 2009; Manga et al., 2009 and references therein). Even distant earthquakes may affect the local hydrology. For example after the 9.3 M Sumatra–Andaman 26 December 2006 earthquake an 11-min swarm of 14 local earthquakes was triggered near Mount Wrangell in Alaska at a distance of ∼ 11,000 km (West et al., 2005), affecting even the water level in ten water wells (Sil and Freymueller, 2006).

Geological structures like faults and anticlines (commonly hosting mud volcanoes) are easily perturbed by earthquakes as they represent weak regions for the seismic wave's propagation. This mechanism is well described by Miller et al. (2004) where earthquakes initiating local fluid movements cause fractures that propagate to the surface manifesting with a time delay from the main earthquake.

4.4. Triggering: seismicity and Lusi

There are several lines of evidence to suggest that the 27th of May 2006 earthquake perturbed venting structures on the Java Island. Besides reactivating faults, the Merapi and Semeru volcanoes (located respectively at 50 and at 270 km from the epicentre of the earthquake) showed stronger activity after the seismic event (Earthobservatory_Nasa, 2006; Harris and Ripepe, 2007; Walter et al., 2007). Of key importance is the intensity of the earthquake recorded in Surabaya (2–3 MMI) and in the northern part of the Arjuno–Welirang volcanic complex (4 MMI) close to the Lusi eruption site (U.S. Geological Survey, 2006). Note that the Watukosek fault originates from the Arjuno–Welirang volcanic complex.

Similarly to what is observed in other settings (e.g. Sil, 2006), the plumbing system in NE of Java was altered by the seismic activity. The record of the wells in the Carat and Tanggulangin fields (both close to Lusi) showed significant changes in pressure soon after the 27-05-2006 earthquake (B. Istadi, pers. comm.). Similarly, 7 min after the quake a pressure loss was observed in the BJP1 well located 200 m away from the eruption site (Sawolo et al., 2009). Additionally, BJP1 experienced a complete loss of circulation 1 h and 20 min after the two aftershocks of the Yogyakarta earthquake (Sawolo et al., 2009). At the same time, villagers witnessed a water

Fig. 10. Schematic cartoon (not to scale) of eruptions along strike-slip faults. The mechanism is applicable for the Lusi eruption events. (A) Shear zone along the Watukosek fault system that crosses Lusi location where a dome-shaped structure existed before the Lusi eruption; (B) activation of the strike-slip fault after the 27-05-2006 earthquake; draining of the fluids from the sedimentary units towards the fault zone; fluids reach the surface using the fault zone as preferential pathway; several craters appears forming an NE–SW oriented alignment coinciding with the fault zone; (C) the mud flow from a prominent crater (later called Lusi) covers all the other eruption sites. The collapse in the region now has an ellipsoidal shape that follows the direction of the Watukosek fault.

Fig. 9. (A) Plot of the effective viscosity profile in the static case ($Vx = 0$ at the sides). Increasing inlet pressure from top to bottom profiles. The lower plot shows the viscosity profile at fluidization. (B–C) Measurements of the critical inlet pressure at fluidization for varying viscosity contrasts, model height and inlet width. The critical pressure normalized by the yield strength collapses onto the same master curve, giving the functional form of ΔP_c (B). Two regimes are obtained. (D) Rescaled critical pressure ΔP_c for moving side boundaries when $(\frac{w}{h})^2 \ll \frac{\mu_2}{\mu_1}$. Negative values on the x-axis denote compression, while positive values denote extension. Different values of parameter α and different viscosity contrasts were studied. (E) Effective viscosity profiles in the presence of tectonic loading. Left part shows compression, while the right part-extension.

level drop of several meters in the wells near Gunung Anyar, and Kalang Anyar mud volcanoes.

Ongoing monitoring at Lusi mud volcano provides a unique record of the response in flow rate to frequent seismicity and periodical fault reactivation (S. Hadi pers. comm.). There are several examples that occurred since the publication of the first series of flow rates (Mazzini et al., 2007). Data gathered during early December 2006 show that after a swarm of earthquakes the mud eruption peaked on December the 6th reaching 160,000 m^3/d. Similarly in the fall 2007, after three months of fluctuating flow rates (varying between 70 and 80.000 m^3/d), two earthquakes (respectively 4.9 and 4.4 M) struck the western coast of Java September 9th 2007 with epicentre almost 200 km away from Lusi (U.S. Geological Survey). The Lusi flow rate increased from 70.000 m^3/d to 120.000 m^3/d after the second earthquake. A flow rate increase of the same order of magnitude was observed after the 10th of October 2007 earthquake with an epicentre 180 km from Lusi. A few hours after this earthquake a 50 m long fracture suddenly appeared along one of the protection dikes framing Lusi generating a vertical displacement of almost 2 m and a lateral shearing of few tens of centimetres (Fig. 4E, F). Interestingly the direction of the fracture and the shearing coincides with the Watukosek fault. This demonstrates that the regional seismic activity is still affecting the motion of the fault. More recently (11th July 2008) a 5.3 earthquake stroke the southwest of Java. A couple of hours later a sudden and unusual kick of smoke and increased flow rate occurred. The following day the situation returned back to normal averages of flow rate. Since the fault-Lusi system does not react to all the seismic events, it is suggested that the system requires time to recharge in order to exhibit significant perturbations.

Numerous of these observations are in contrast with Tingay et al. (2008) that proposed a model to test the stress induced by the earthquake on the Watukosek fault. The authors concluded that the 2006 Yogyakarta earthquake was too weak to reactivate faults at this distance. However these results were obtained using earthquake intensity values of 2 rather than the actual 4 recorded close to the Arjuno–Welirang volcanic complex (U.S. Geological Survey, 2006). Moreover this model neglects many factors that can simultaneously affect a system in critical conditions (and hence the fault reactivation) such as the actual stress already present in the fault, the influence of the overpressured fluids in the system, and the possible influence of the Penanggungan volcano in affecting the local plumbing system. Finally the presence of the shearing due to the fault reactivation is not considered in their model, which is the key point of our hypothesis. Manga (2007) compiled a collection of supposedly earthquake-induced eruptions. Their conclusion is that the Lusi eruption fall outside the main statistical cluster and therefore a possible link with the Yogyakarta earthquake is unlikely. However these conclusions are done on (1) cluster analyses and (2) consider mud volcanoes that already exist and that have a periodic activity. It is well known that most mud volcanoes during their dormant period (i.e. the interval separating one eruption from another) have a constant fluid release from the crater; hence a pressure build-up at depth is slower due to the constant fluid release through the pre-existing channel network. Therefore already existing mud volcanoes require a stronger shaking to trigger a possible eruption compared to newly born structures. Indeed the Lusi mud volcano, to our knowledge, represent the first and only mud volcano that is studied from its' birth and hence cannot be treated in statistical analyses together with structures that already have a long eruption history. Above all, Tingay et al. (2008) and Manga (2007) do not consider that at Lusi site was already existing a piercement structure (as documented by seismic data) prone to manifest to the surface. Hence the approaches described in their studies differs substantially from the data described hereby.

4.5. Drilling as a trigger?

The hypothesis of an eruption caused by the drilling of BJP1 well was initially proposed by the media immediately after the eruption and later reiterated by Davies et al. (2007). However the hypothesis presented by these authors was almost entirely based on the limited amount of publicly available data at the time. Davies et al. (2008) and Tingay et al. (2008) proposed a similar mechanism to explain the man-made hypothesis based on the interpretation of drilling data without considering the geological setting (fault zone, existing piercement structure). The conclusion was that the formation strength around the well was exceeded when the blowout preventers were closed causing hydrofracturing at the casing shoe and a consequent eruption. This conclusion has been challenged by e.g. Nawangsidi (2007) and Sutriono (2007). Sawolo et al. (in this issue) question the "man-made" hypothesis providing an alternative interpretation of the drilling data. It is not the purpose of our article to investigate the drilling data that are currently being discussed by several authors. A few key observations should be highlighted regarding the "man-made" hypothesis debate:

- The close distance between the BJP1 well and the Lusi crater might not be a coincidence.
- Likewise it might not be a coincidence that the drilling mud losses occurred after the earthquake and its aftershocks.
- No evidence of an underground blow-out was observed from or around the BJP1 well (classic blow-out scenario).
- No kick was recorded in the deepermost part of the borehole, instead mud losses were recorded which coincided with the timing of the earthquake. One day later, a kick was taken while pulling out the drilling assembly at a depth of 1290 m. Although the origin of this sudden pressure increase is still unknown, it is probable that this was connected with the reactivation of the Watukosek fault.
- Cuttings from the deepermost part of the BJP1 well did not reveal the presence of any carbonate (supposedly coming from the Kujung Formation), and calcimetry data indicate only 4% calcite with no significant increase or changes.

Furthermore we emphasize that a) initially the eruption was distributed through six different seepage points, b) the Watukosek fault, and its faults system, is crossing the area exactly in this location, and that c) the projection to the surface of the top part of the piercing feature observed in the seismic lines (Fig. 6) coincides with the actual Lusi crater. A sole man-made drilling hypothesis would find difficult to explain the numerous aligned craters that appeared during the initial eruption phase. If hydrofracturing was triggered at depth during the drilling operations, only a single surface eruption or a sparser distribution of the eruptions around the well would be expected.

5. Conclusions

Seismic interpretation reveals that a fault zone (Watukosek) and a dome were located at the Lusi site before the eruption. Field evidence shows that the strike-slip Watukosek fault was reactivated after the earthquake of the 27th of May 2006. The shear movement along the fault perturbed the geological setting likely affecting the precarious equilibrium of overpressured units allowing fluids to be flushed along the fault pathway. These fluids ultimately reached the surface at several locations aligned in NE–SW direction around the Lusi site. Simultaneously an increased seepage activity of other pre-existing mud volcanoes was observed in the NE of Java.

In order to corroborate these regional observations, analogue laboratory experiments, and a set of mathematical modeling for brittle and ductile rheologies were completed. The experiments show that fluidization occurs along the imposed shear zone where the critical fluid pressure is reduced. This observation is also supported by the mathematical modeling for ductile rheologies. The results show that the critical fluid pressure is reduced for increasing horizontal stresses. Additionally, the same shear-induced fluidization mechanism is obtained in the model for brittle rheologies when equating the differential stress and both the Mohr-Coulomb and von Mises failure criterions. All these independent methods demonstrate that shearing is an efficient mechanism for triggering the eruptions in naturally prepared settings. Given a fluid over pressure at depth, localization of tectonic stresses may induce fluidization in situation that would otherwise be stable. This mechanism is applicable to several geological settings where shear zones host piercement structures.

Strong evidence published to date supports the natural trigger mechanism, however a human contribution cannot be totally discarded. The significance of the neighboring BJP1 well in the Lusi eruption is debated. At the time of this writing, the interpretation of the drilling data is far from being settled. Based on the evidence described in this manuscript, it seems unlikely that the sole BJP1 well was able to alter the plumbing system at a regional scale reactivating the Watukosek fault that crosses the NW part of Java.

The data and observations described here show that all the ingredients required for mud volcano activity are present in the NE of Java. The conditions for the extensive mud volcanism on Java result from natural geological processes often involving over-pressure release along faults.

Acknowledgements

Appendix 1

Modeling of ductile rheology

A Bingham material has a high viscosity μ_1, simulating a strong material, or a solid, until the differential stress reaches a critical value τ_c at which the viscosity drops to μ_2 and the material has a fluid-like behaviour. This viscosity drop is in essence our approach to model the process of fluidization as a solid-fluid phase transition. The effective viscosity $\mu_{\text{effective}}$ used in the numerical code can be computed both as a function of second stress invariant and second strain rate invariant. In the modeling presented here the calculation of the effective viscosity $\mu_{\text{effective}}$ used the second strain rate invariant according to the formula

$$\mu_{\text{effective}} = \begin{cases} \mu_1 & \dot{\epsilon} < \dot{\epsilon}_c \\ \mu_2 + \frac{\dot{\epsilon}_c(\mu_1 - \mu_2)}{\dot{\epsilon}} & \dot{\epsilon} \geq \dot{\epsilon}_c \end{cases} \tag{1}$$

The Bingham fluid is a non-linear material since the rheology

depends on the stresses. This study focused on the rheological effects of the differential stresses to understand the process of fluidization. To solve the non-linear system of equations the Picard (simple) iterations were used (Press et al., 1992). In this approach every iteration starts with running a linear, incompressible viscous Stokes solver with a variable viscosity. Velocity and stress fields are computed for given boundary conditions and effective viscosity, as described in Dabrowski et al. (2008). Subsequently the material viscosity is updated according to the formula (1), which completes a single iteration. The whole process is repeated until changes in the effective viscosity are below a specified threshold. The result of this procedure is an effective viscosity profile within the box.

Appendix 2

Brittle rheology results

The yield strength of mud have been previously modeled by the von Mises failure criterion where the shear strength of the material equals a constant value τ_c (Imran et al., 2001; Marr et al., 2002). The critical fluid pressure at depth causing the formation of the piercement structure is defined when the differential stress equals τ_c,

$$\tau = \tau_c \tag{2}$$

where the differential stress is given by

$$\tau^2 = \frac{1}{6}\left[(\sigma_{xx} - \sigma_{yy})^2 + (\sigma_{yy} - \sigma_{zz})^2 + (\sigma_{zz} - \sigma_{xx})^2\right] + \sigma_{xy}^2 + \sigma_{yz}^2 + \sigma_{zx}^2 \tag{3}$$

The stress-directions are defined in Fig. 3B corresponding to the experimental setup.

Terzaghi (1943) described the effects of the fluid pressure in rocks and in particular the weakening effect of the fluid pressure. Since then, several other authors investigated the effect of seepage forces due to gradients in the fluid pressure on the local stress field (e.g. Mourgues and Cobbold, 2003; Cobbold and Rodriguez, 2007; Rozhko, 2007; Rozhko et al., 2007). In these models the authors defined the vertical stress as the lithostatic weight minus the fluid pressure ΔP

$$\sigma_{zz} = \rho gh - \Delta P \tag{4}$$

where ρ is the density, g is the gravity, h represents the sediment thickness, and ΔP is the fluid pressure difference between the surface and the considered depth. The horizontal stresses in the x and y direction are equal and given by a constant coefficient (κ) times the vertical stress

$$\sigma_{xx} = \sigma_{yy} = \kappa \sigma_{zz} \tag{5}$$

where κ is the coefficient of side stresses that defines how much of the vertical stress propagate into the horizontal direction. κ can vary between zero and one. In the laboratory experiment, the shear stress was induced by pulling the plastic net localizing the shear stress along the shear zone. According to the definition of the stress direction in Fig. 3B, the only non-zero shear stress was on the x-plane in the y-direction.

With the given model for the stresses included into the deviatoric stress and the assumption of the von Mises failure criterion it is possible to solve the equation for the critical fluid pressure difference,

$$\frac{\Delta P_c}{\tau_c} = \frac{\rho g h}{\tau_c} + \frac{\sqrt{3}}{1 - \kappa} \sqrt{1 - \frac{\sigma_{xy}^2}{\tau_c^2}} \tag{6}$$

Equation (6) shows that the critical fluid pressure depends on the lithostatic weight plus a material-dependent yield function. This function is reduced by the non-zero shear stresses. The analysis also shows that when the shear stresses are equal to the yield strength of the material, the critical fluid pressure at fluidization ΔP_c is at the minimum.

Frictional materials, such as, e.g. granular matter and also sedimentary rocks, have previously shown to follow a more complex rheology. In this model the shear strength is no longer a constant but proportional to the loading. This behaviour is modeled by the use of Mohr-Coulomb rheology (Paterson and Wong, 2005) where the yield Y_{M-C} strength is given by,

$$Y_{M-C} = C + \frac{(\sigma_{zz} - \sigma_{xx})}{2} \sin \phi \tag{7}$$

where C is the cohesion and ϕ is the internal angle of friction. The stresses are modeled using the same approach as for the von Mises criterion using Equations (4) and (5). By equating the yield function with the differential stress at fluidization, we solved the equation for the critical fluid pressure difference,

$$\frac{\Delta P_c}{C} = \frac{\rho g h}{C} + \frac{\sin \phi - \frac{2}{3}\sqrt{1 - \frac{\sigma_{xy}^2}{C^2}\cos^2 \phi}}{(1 - \kappa)\left(\frac{2}{3} - \sin^2 \phi\right)} \tag{8}$$

The Equation (8) shows that the critical fluid pressure at fluidization ΔP_c is reduced for increasing shear stresses σ_{xy}.

Appendix 3

Ductile rheology modeling: no tectonic loading

For the reference case with no tectonic loading at the model boundaries, the data collapsed onto a single master curve for varying viscosity ratios, critical stress, inlet width and the model height. The critical fluidization pressure is described by the following equations for two distinct regimes:

$$\frac{\Delta P}{\tau_c}\Big|_c \cong \begin{cases} 20\frac{\mu_2}{\mu_1}\left(\frac{h}{w}\right)^2 & \text{for } \frac{\mu_1}{\mu_2}\left(\frac{w}{h}\right)^2 \ll 1 \\ 10 & \text{for } \frac{\mu_1}{\mu_2}\left(\frac{w}{h}\right)^2 \gg 1 \end{cases} \tag{9}$$

Assuming some transient regime for $\left(\frac{w}{h}\right)^2 \approx \frac{\mu_2}{\mu_1}$. The second regime is selected considering the ratio inlet width/depth $\frac{w}{h} \approx 0.01$ (a low end estimate) and the ratio of the viscosity before and after fluidization $\frac{\mu_1}{\mu_2} \approx 10^6$ (a low end estimate). The corresponding value of ΔP_c is ~ 10 times the material yield strength τ_c (Fig. 9C). Further increase of viscosity ratio and the aspect ration towards more realistic values will maintain the same regime and the same fluid overpressure value. To conclude, in the case of no tectonic loading the model predicts high fluid overpressure regardless of the poorly constrained viscosity ratio. Fig. 9D shows how this high value can be significantly lowered in the presence of tectonic forcing.

Appendix 4

Background geology

A few points are relevant to emphasise regarding the stratigraphy of the region around Lusi in the backark basin of NE Java.

These details highlight why this region is prone to mud volcanism. More information can be found in Mazzini et al. (2007).

- The whole basin is characterized by high sedimentation rates of water saturated sediments (e.g. at Lusi location equal to 2.5 km/my since the Pleistocene).
- The subduction of the oceanic plate to the south triggers earthquakes along the subduction zone that in turn causes misbalances in the backark sedimentary basin.
- Layers of organic-rich sediments (mainly clay) present in the sedimentary sequence are excellent for hydrocarbon generation and are capped by units of volcaniclastic sand that form a good seal.
- Overpressured units within the bluish grey clays (Upper Kaliberg Fm.) commonly indicate presence of hydrocarbons.
- The closely located Arjuno–Welirang volcanic complex creates a generally high geothermal gradient (~ 42 °C/km). This high gradient allows mineralogical and geochemical transformations that normally occur at greater depths.
- The illitization of clays, that in ordinary basins takes place at depth of 2.5–5 km, is already occurring at 1100 m at Lusi (and possibly shallower). This mineralogical reaction results in a significant release of interstitial fluids of the clay minerals that contribute, together with the hydrocarbon generation, to the overpressure (e.g. Perry and Hower, 1972).

All these bullets are considered as efficient causes to develop the observed mud volcanism on Java.

References

Bonini, M., 2007. Interrelations of mud volcanism, fluid venting, and thrust-anticline folding: Examples from the external northern Apennines (Emilia-Romagna, Italy). Journal of Geophysical Research 112, B08413, doi:10.1029/2006JB004859.

Brown, K.M., 1990. The nature and hydrogeologic significance of mud diapirs and diatremes for accretionary systems. Journal of Geophysical Research 95 (B6), 8969–8982.

Chigira, M., Tanaka, K., 1997. Structural features and history of mud volcanoes in southern Kokkaido, northern Japan. Journal – Geological Society of Japan 103, 781–793.

Cobbold, P.R., Rodriguez, N., 2007. Seepage forces, important factors in the formation of horizontal hydraulic fractures and bedding-parallel fibrous veins ('beef' and 'cone-in-cone'). Geofluids 7 (3), 313–322.

Dabrowski, M., Krotkiewski, M., W., S.D., 2008. MILAMIN: MATLAB-based finite element method solver for large problems. Geochemistry, Geophysics, Geosystems 9, Q04030, doi:10.1029/2007GC001719.

Davies, R., Swarbrick, R., Evans, R., Huuse, M., 2007. Birth of a mud volcano: east Java, 29 may 2006. GSA Today 17, 4–9.

Davies, R.J., Brumm, M., Manga, M., Rubiandini, R., Swarbrick, R., Tingay, M., 2008. The East Java mud volcano (2006 to present): an earthquake or drilling trigger? Earth and Planetary Science Letters 272 (3–4), 627–638.

Delisle, G., 2004. The mud volcanoes of Pakistan. Environmental Geology 46, 1432–1495.

Delisle, G., von Rad, U., Andruleit, H., van Daniels, C., Tabreez, A., A., I., 2002. Active mud volcanoes on- and offshore eastern Makran, Pakistan. International Journal of Earth Sciences 91 (1), 93–110.

Dia, A.N., Castrec-Rouelle, M., Boulegue, J., Comeau, P., 1999. Trinidad mud volcanoes: where do the expelled fluids come from? Geochimica et Cosmochimica Acta 63 (7–8), 1023–1038.

Earthobservatory_Nasa, 2006. http://earthobservatory.nasa.gov/NaturalHazards/natural_hazards_v2.php3?img_id=13607.

Eggert, S., Walter, T.R., 2009. Volcanic activity before and after large tectonic earthquakes: observations and statistical significance. Tectonophysics 471, 14–26.

Ellouz-Zimmermann, N., Lallemant, S.J., Castilla, R., Mouchot, N., Leturmy, P., Battani, A., Buret, C., Cherel, L., Desaubliaux, G., Deville, E., Ferrand, J., Lügcke, A., Mahieux, G., Mascle, G., Mühr, P., Pierson-Wickmann, A.C., Robion, P., Schmitz, J., Danish, M., Hasany, S., Shahzad, A., Tabreez, A., 2007. Offshore frontal part of the Makran accretionary prism (Pakistan): the CHAMAK survey. In: Lacombe, O., Roure, F. (Eds.), Thrust Belts and Foreland Basins. Special Volume. Springer-Verlag, pp. 349–364 (Chapter 18).

Fukushima, Y., Mori, J., Hashimoto, M., Kano, Y., 2009. Subsidence associated with the LUSI mud eruption, east Java, investigated by SAR interferometry. Marine & Petroleum Geology 26, 1740–1750.

Gidaspow, D., 1994. Multiphase Flow and Fluidization. Academic Press Inc. Harcourt Brace & Company, 457 pp.

Guliev, I.S., Feizullayev, A.A., 1997. All about Mud Volcanoes. Nafta Press, Baku, 52 pp.

Harris, A.J.L., Ripepe, M., 2007. Regional earthquake as a trigger for enhanced volcanic activity: evidence from MODIS thermal data. Geophysical Research Letters 34, L02304, doi:10.1029/2006GL028251.

Hieke, W., 2004. The August 27, 1886 earthquake in Messenia (Peloponnesus) and reported flames over the Ionian Sea–a Mediterranean Ridge gas escape event? Marine Geology 207 (1–4), 259–265.

Imran, J., Harff, P., Parker, G., 2001. A numerical model of submarine debris flows with graphical user interface. Computers Geosciences 274 (6), 717–729.

Istadi, B., Pramono, G.H., Sumintadireja, P., Alam, S. Simulation on growth and potential Geohazard of East Java Mud Volcano, Indonesia. Marine & Petroleum Geology, Mud volcano special issue, doi: 10.1016/j.marpetgeo.2009.03.006.

Jakubov, A.A., AliZade, A.A., Zeinalov, M.M., 1971. Mud Volcanoes of the Azerbaijan SSR. Atlas. Azerbaijan Academy of Sciences, Baku (in Russian).

Judd, A., Hovland, M., 2007. Seabed Fluid Flow. Cambridge University Press, Cambridge, 475 pp.

Kopf, A.J., 2002. Significance of mud volcanism. Review of Geophysics 40 (2), 1–52.

Kopf, A.J., 2008. Volcanoes: making calderas from mud. Nature Geoscience 1 (8), 500–501.

Lemarchand, N., Grasso, J.R., 2007. Interactions between earthquakes and volcano activity. Geophysical Research Letters 34 (24), L24303.

Linde, A., Sacks, I.S., 1998. Triggering of volcanic eruptions. Nature 857, 888–890 (395(6705)).

Manga, M., 2007. Did an earthquake trigger the may 2006 eruption of the Lusi mud volcano? EOS 88 (18), 201.

Manga, M., Brodsky, E., 2006. Seismic triggering of eruptions in the far field: volcanoes and geysers. Annual Review of Earth and Planetary Sciences 34, 263–291.

Manga, M., Rudolph, M.L., Brumm, M., 2009. Earthquake triggering of mud volcanoes: a review 26, 1785–1798.

Marr, J.G., Elverhøi, A., Harbitz, C., Imran, J., Harff, P., 2002. Numerical simulation of mud-rich subaqueous debris flows on the glacially active margins of the Svalbard-Barents Sea. Marine Geology 188 (3–4), 351–364.

Mau, S., Rehder, G., Arroyo, I.G., Gossler, J., Suess, E., 2007. Indications of a link between seismotectonics and CH$_4$ release from seeps off Costa Rica. Geochemistry, Geophysics, Geosystems 8 (4), 1–13.

Mazzini, A., Svensen, H., Akhmanov, G.G., Aloisi, G., Planke, S., Malthe-Sorenssen, A., Istadi, B., 2007. Triggering and dynamic evolution of the LUSI mud volcano, Indonesia. Earth and Planetary Science Letters 261 (3–4), 375–388.

Mazzini, A., Svensen, H., Planke, S., Guliyev, I., Akhmanov, G.G., Fallik, T., Banks, D., 2009. When mud volcanoes sleep: insight from seep geochemistry at the Dashgil mud volcano, Azerbaijan. Marine and Petroleum Geology, doi:10.1016/j.marpetgeo.2008.11.003.

Mellors, R., Kilb, D., Aliyev, A., Gasanov, A., Yetirmishli, G., 2007. Correlations between earthquakes and large mud volcano eruptions. Journal of Geophysical Research 112, B04304.

Miller, S.A., Cristiano, C., Chiaraluce, L., Cocco, M., Barchi, M., Kaus, B.J.P., 2004. Aftershocks driven by a high-pressure CO$_2$ source at depth. Nature 427, 724–727.

Mourgues, R., Cobbold, P.R., 2003. Some tectonic consequences of fluid overpressures and seepage forces as demonstrated by sandbox modeling. Tectonophysics 376, 75–97.

Nakamukae, M., Haraguchi, T., Nakata, M., Ozono, S., Tajika, J., Ishimaru, S., Fukuzumi, T., Inoue, M., 2004. Reactivation of the Niikappu mud volcano following the Tokachi-oki earthquake in 2003. Japan Earth and Planetary Science 2004 (Joint meeting, Chiba, Japan).

Nawangsidi, D., 2007. Drilling and Mud Flow at Lusi Mud Volcano. International Geological Workshop on Sidoarjo Mud Volcano, Jakarta (February 2007).

Paterson, M.S., Wong, T.F., 2005. Experimental Rock Deformation – The Brittle Field, 2nd ed. Springer-Verlag, Berlin, Heidelberg, New York, 348 pp.

Perry, E.A., Hower, J., 1972. Late-stage dehydration in deeply buried pelitic sediments. AAPG Bulletin 56 (10), 2013–2021.

Planke, S., Svensen, H., Hovland, M., Banks, D., Jamtveit, B., 2003. Mud and fluid migration in active mud volcanoes in Azerbaijan. Geo-Marine Letters 23, 258–268.

Press, W.H., Teukolsky, S.A., Vetterling, W.T., B.P., F., 1992. Numerical Recipes in C: the Art of Scientific Computing. Cambridge University Press, New York, NY, USA, ISBN 0521437148.

Rozhko, A., 2007. Role of seepage forces on hydraulic fracturing and failure patterns. PhD thesis, University of Oslo and University of Grenoble.

Rozhko, A., Podladchikov, Y.Y., Renard, F., 2007. Failure patterns caused by localized rise in pore-fluid overpressure and effective strength of rocks. Geolphysical Research Letters 34.

Sawolo, N., Sutriono, E., Istadi, B., Darmoyo, A.B., 2009. The LUSI mud volcano triggering controversy: was it caused by drilling? Marine & Petroleum Geology 26, 1766–1784.

Sil, S., 2006. Response of Alaskan well to near and distant large earthquakes. M.Sc thesis, University of Alaska Fairbanks, 92.

Sil, S., Freymueller, J.T., 2006. Well water level changes in Fairbanks, Alaska, due to the great Sumatra-Andaman earthquake. Earth Planets Space 58, 181–184.

Sutriono, E., 2007. Drilling Operations at Lusi Site. International Geological Workshop on Sidoarjo Mud Volcano, Jakarta (February 2007).

Terzaghi, K., 1943. Theoretical Soil Mechanics. John Wiley and Sons, New York, 528 pp.

Tingay, M.R.P., Heidbach, O., Davies, R., Swarbrick, R., 2008. Triggering of the Lusi Mud Eruption: Earthquake Versus Drilling Initiation. Geology, vol. 36(8), pp. 639–642.

U.S. Geological Survey. http://earthquake.usgs.gov/eqcenter/.

U.S. Geological Survey, 2006. http://earthquake.usgs.gov/eqcenter/eqinthenews/2006/usneb6/.

Walter, T.R., Amelung, F., 2007. Volcanic eruptions following M $\geq$ 9 megathrust earthquakes: implications for the Sumatra-Andaman volcanoes. Geology 35 (6), 539–542.

Walter, T.R., Wang, R., Zimmer, M., Grosser, H., Lühr, B., Ratdomopurbo, A., 2007. Volcanic activity influenced by tectonic earthquakes: static and dynamic stress triggering at Mt. Merapi. Geophysical Research Letters 34, L05304.

West, M., Sanchez, J.J., McNutt, A.R., 2005. Periodically triggered seismicity at Mount Wrangell, Alaska, after the Sumatra Earthquake. Science 308, 1144–1146.